A Study on Nozzle Flow Quality of Low Power Arcjet Thruster for Improvement of Propulsion Efficiency

S.ASO,K.TAKAYANAGI,S.KUTI-ISHI and K.SUGIMOTO
Department of Aeronautics and Astronautics,Kyushu University

Contact person: Dr.shigeru ASO;6-10-1 Hakozaki,Higashi-ku,Fukuoka 812-8581,JAPAN
tel:81-92-642-3747 fax:81-92-642-3752 e-mail:aso@aero.kyushu-u.ac.jp presentation:Oral

1. Introduction

Now, space activity is coming to be more active than ever, for example lunching larger satellites, building space station and traveling between planets etc.
In general, the electric thruster is the propulsion systems which convert electric energy to physical energy. The primary merit of electric thrusters for spacecraft is highly efficient use of propellant mass.

Highly efficient use of propellant mass is made by high exhaust speed. This gives greater reduction of the spacecraft's weight and the achievement of space missions, which is impossible by using conventional chemical rockets. These electric propulsion is used not only for interplanetry missions, but also for various satellites missions around earth due to long life span.
DC-Arcjet Thruster is one of the electric propulsion systems and used mainly for orbit control of satellites around earth. However, for the design of DC-Arcjet Thruster the inside flow field of the thruster has not been understand sufficiently. The flow field of the thruster is so complicated because of exitence of plasma, electric field and magnetic field. In the present study numerical analysis on the inside flow field of low power Arcjet Thrusters has been conducted. Especially the voscosity effect of the nozzle on the propulsion efficiency is studied. [1]

2. Structure of DC-Arcjet Thruster

The schematic of typical DC-Arcjet Thruster is shown in Fig.1. DC voltage is charged between anode and cathode and produces arc between them. Propellant that flows into nozzle from upstream at subsonic speed is heated by electric discharge, which is produced between cathode and anode. The heated propellant has high enthalpy condition and produces the Arc Column. At this situation, particles of propellant is dissociated and ionized. And, propellant is accelerated gas dynamically into supersonic speed through the nozzle.

3. Method of Numerical Analysis

3.1 Governing Equation

The fundamental two-dimensional equations, which hold at thermal and chemical nonequilibrium state, are as follows.

1) Equation for conservation of total mass
2) Equation of axial momentum
3) Equation of radial momentum
4) Equation for conservation of total energy
5) Equation for conservation of mass of each species
6) Equation for conservation of vibrational energy
7) Equation for conservation of electron energy

Following equations are representative of each equation in tensor. All symbols follow the established procedures.

$$\frac{\partial q}{\partial t}+\frac{\partial F_k}{\partial x_k}=S$$

$$q=\begin{bmatrix}\rho\\ \rho u_1\\ \rho u_2\\ E\\ \rho_1\\ \vdots\\ \rho_{ns}\\ e_{vib}\\ e_e\end{bmatrix} \qquad F_k=\begin{bmatrix}\rho u_k\\ \rho u_1 u_k+\delta_{1,k}p-\tau_{k,1}\\ \rho u_2 u_k+\delta_{2,k}p-\tau_{k,2}\\ (E+p)u_k-\tau_{t,k}\\ \rho_1 u_k-\rho D_1\dfrac{\partial}{\partial x_k}X_1\\ \vdots\\ \rho_{ns}u_k-\rho D_{ns}\dfrac{\partial}{\partial x_k}X_1\\ e_{vib}u_k-\tau_{vib,k}\\ e_e u_k-\tau_{e,k}\end{bmatrix}$$

$$S=\begin{bmatrix}0\\ 0\\ 0\\ 0\\ \dot{\omega}_1\\ \vdots\\ \dot{\omega}_{ns}\\ S_{vib}\\ S_e\end{bmatrix}$$

Those equations are converted into axisymetric equations.

$\tau_{k,i}$ denotes stress-strain tensor, and each of $\tau_{t,k},\tau_{vib,k},\tau_{e,k}$ denotes total energy, vibrational energy and, viscosity loss of electron energy. And $\dot{\omega}_s$ denotes the genesis-disappearance term by chemical reaction about species of.

$$S_{vib}=\sum_{s=molecule}\rho_s\frac{e^{eq}_{vib,s}(T)-e_{vib,s}(T_{vib})}{\langle\tau_s\rangle}+\rho_{N_2}\frac{e^{eq}_{vib,N_2}(T_e)-e_{vib,N_2}(T_{vib})}{\tau_e}+\sum_{i=M}\tilde{E}_{D,i}\dot{\omega}_i^D$$

The first term of right hand is the rate of energy exchange between translational and rotational energy, the second term is the rate of energy exchange between vibration and electron energy, and the third term is the production-dissipation term for vibrational energy due to dissociation. And as for energy exchange between vibrational and electron energy, we assume only nitrogen molecules.

$$S_e=3\rho_e(T-T_e)\sum_{s\neq e}(1+g_{rot,s})\nu_{e,s}R_s-\rho_{N_2}\frac{e^{eq}_{vib,N_2}(T_e)-e_{vib,N_2}(T_{vib})}{\tau_e}+E_{I,N}\dot{\omega}^e_N+E_{D,N_2}\dot{\omega}^e_{N_2}-p_e\frac{\partial u_l}{\partial x_l}$$

The first term of right hand is the rate of energy exchange between translational mode and electron mode, the second term is the rate of energy exchange between rotational mode and electron mode, the third term is the production-dissipation term of electron energy by electron impact dissociation, the fourth term is the production-dissipation term of electron energy by electron impact ionization, and the fifth term is the component of the convection term for electron pressure.

3.2 The Model of The Flow Field

In the present analysis the model of the flow field is assumed as follows.

1) The propellant is nitrogen.
2) Continuous flow
3) Laminar flow
4) Axisymmetric flow
5) Ignoring the effect of electric field and magnetic field
6) Thermal and chemical nonequilibrium flow
7) 5 species $(N_2, N, N_2^+, N^+, e^-)$
8) One temperature model
9) Ignoring the energy mode of electron excitation
10) The vibrational temperature of all molecules is equal.
11) The effect of radiation is neglected.

3.3 Chemical Reaction Models

In the present calculation we assumed 5 species and 8 chemical reactions, and those chemical reaction models are as follows.

- ○ Heavy Particle-Impact Dissociation
  $N_2 + M \Leftrightarrow N + N + M \quad (M = N_2, N, N_2^+, N^+)$
- ○ Electron-Impact Dissociation
  $N_2 + e^- \Leftrightarrow N + N + e^-$
- ○ Associative Ionization
  $N + N \Leftrightarrow N_2^+ + e^-$
- ○ Charge Exchange
  $N_2 + N^+ \Leftrightarrow N_2^+ + N$
- ○ Electron-Impact Ionization
  $N + e^- \Leftrightarrow N^+ + e^- + e^-$

3.4 Nozzle Shape and Computational Grid

The representative nozzle geometry is shown in Fig.2. The computational Grid of the nozzle is shown in Fig.3.

3.5 Inflow Condition

This numerical production code dose not contain the production terms of Joule heating by discharging. So in order to estimate the gas temperature after arc heating for initial condition, we assumed physical model as showing in Fig.4. In the model the propellant(stagnation temperature: T_0) is heated by Joule-heating up to the stagnation temperature of T_0^*. The mechanism is expressed as follows:

where

$$\dot{m}c_p T_0 + \eta P = \dot{m}c_p T_0^*$$

$\dot{m}$:mass flow rate

c_p :specific heat at constant pressure

P :charging electric power

η :thermal efficiency

We use T_0^* as the stagnation temperature of the propellant.

3.6 Boundary Condition

At nozzle exit out-flow boundary condition with zero derivative with respect to x(main flow direction) is used. The nozzle wall is assumed as adiabatic and non-slip

4. Results and Discussions

4.1 A study on the viscosity effect of the small nozzle

Usually the throat of low power Arcjet Thruster is very small, such as below 0.3[mm]. Due to the such a small throat, the whole flow field might be influenced significantly by viscosity. In order to evaluate the viscous effect, we calculate the flow of Fig.2(Case 1). Also we calculate the flow of the nozzle(Case 2), whose size is 100 times as large as that of Fig.2.

In order to make the charging energy per unit mass equal for both cases, we set its mass flow rate and charging electric power of Case 2 10^4 times as much as Case 1. Actual testing conditions are shown in Table.1.

The inflow temperature is determined by the flow model of Fig.4. Velocity distributions are shown in Fig.5 and Fig.6. The Mach number and density distributions at each nozzle exit are shown in Fig.7 and Fig.8.

Comparing Fig.5(Case 1) with Fig.6(Case 2), we can see clearly that the potential nozzle core of Case 1 is much smaller than that of Case 2. Also we find in Case 1 that boundary layer covers most of the nozzle region. Those results show that the viscosity effect very significant for the small nozzle geometry such as Low Power Arcjet Thruster.

On the other hand, in Case 2(Fig.6) the boundary layer similarly grows on the surface of the wall.

As the nozzle is enough large. Then the boundary layer does not block the nozzle flow fully accelerated. In short, the distance from a surface of wall to the potential nozzle core is very short in a small nozzle such as Case 1 and the distance is enough large in a large nozzle such as Case 2. In other words, the area ratio of the

boundary layer for propellant flow is large in a small nozzle and small in a large nozzle.

Specific Impulse(ISP) and Reynolds number are shown in Table.2. Reynolds number is calculated based on nozzle exit diameter, and calculated flow properties at nozzle throat. The Reynolds number of Case 2 is about 100 times as large as that of Case 1. From the stand point of Reynolds number, we can expect that the viscosity effect of Case 1 is much larger than that of Case 2.

The results show for small nozzle whose diameter of the throat is about 0.3[mm] the nozzle performance, such as Isp, becomes worse than that of potential flow prediction due to viscous effect.

4.2 A study of the effect of the nozzle throat diameter on the performance of the thruster for the small nozzle

For the study the throat diameter is changed as shown in Table.3 and those performances are compared. We assumed the mass flow rates and the inflow temperatures of 3 cases are equal. In order to keep mass flow rate for different nozzle throat, the only inflow pressure is different.

Fig.9 and Fig.10 show each velocity distribution. Fig.11 and Fig.12 show each Mach number and density distribution at the nozzle exit. The diameter of the throat, specific impulse(ISP) and Reynolds number of Case 1,3,4 are shown in Table.4

Comparing Figs.5,9,10, the boundary layer covers most of the nozzle region and there are little difference of core size of potential nozzle flows for 3 cases.

However, Mach number distributions and density distributions of Case 1,3,4 are different near the nozzle axis. Mach number and density at nozzle axis become large as the diameter of the throat is decreased. The reason is follows:

Isp becomes large. As the diameter of the throat is decreased. The core density becomes large, while the core velocity keep almost constant.

However, there may be some optimal minimum diameter of the throat. The stagnation pressure should be increased when the diameter of the throat is decreased in order to keep the same mass flow rate. However, for higher stagnation pressure, electric discharge becomes difficult.

5. Conclusions

The conclusions of the present study are summarized as follows.

1) In the inside flow field of the low power Arcjet Thruster the viscosity effect is very large and the boundary layer covers most of the nozzle region. This viscosity effect has a great influence on Isp.

2) For same inflow temperature and mass flow rate, the core density becomes larger and core velocity keep almost constant as the diameter of the nozzle is decreased. Then, Isp becomes larger. The nozzle which has the shorter diameter of the throat has a little larger thrust by difference of the core's density although there is little difference of each velocity.

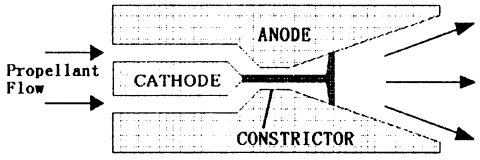

Fig.1 schematic digram of DC-Arcjet Thruster

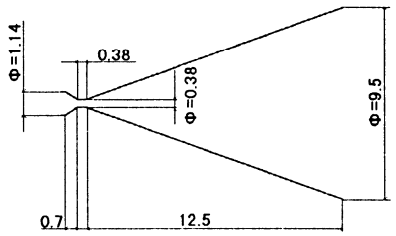

Fig.2 shape of nozzle (Grid-1)

Fig.3 Grid-1(135×40)

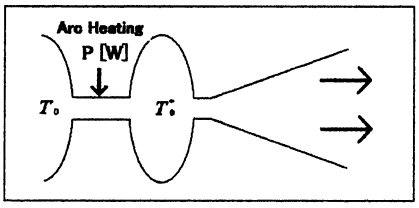

Fig.4

	Case 1	Case 2
P [W]	500	500×10^4
η	0.3	0.3
Diameter of Throat [mm]	0.38	0.38×10^2
$\dot{m}$ [kg/s]	3.0×10^{-5}	3.0×10^{-1}
T_0^* [K]	5110	5110

Table.1

Fig.5 velocity (Case 1)

Fig.6 velocity (Case 2)

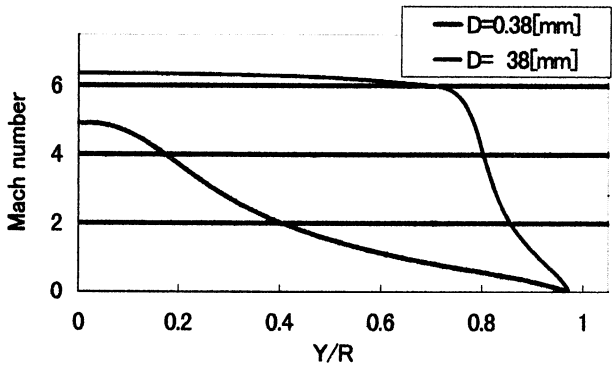

Fig.7 Mach number

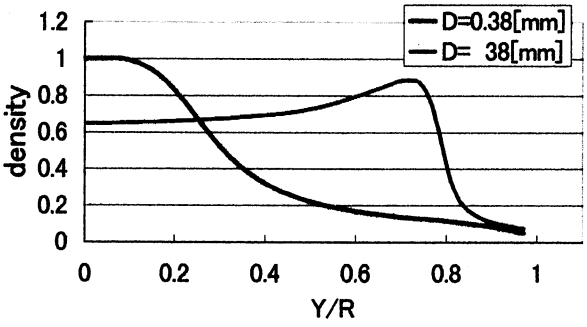

Fig.8 density

	Case 1	Case 2
ISP	301	336
Reynolds number	1280	11500

Table.2

	Case 1	Case 3	Case 4
Diameter of Throat [mm]	0.380	0.538	0.310
P [W]	500	500	500
η	0.3	0.3	0.3
$\dot{m}$ [kg/s]	3.0×10^{-5}	3.0×10^{-5}	3.0×10^{-5}
T_0^* [K]	5110	5110	5110

Table.3

Fig.9 velocity (Case 3)

Fig.10 velocity (Case 4)

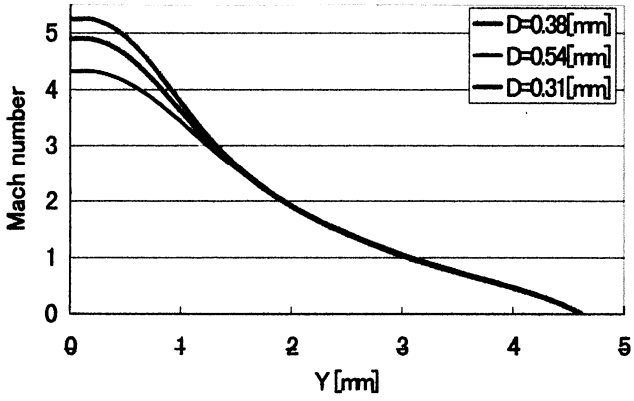

Fig.11 Mach number

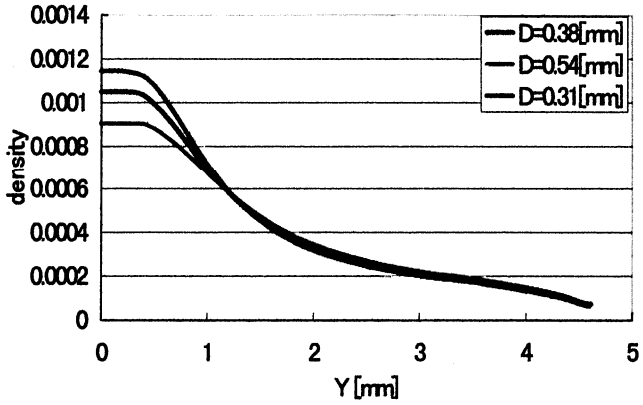

Fig.12 density

	Case 4	Case 1	Case 3
Diameter of Throat [mm]	0.31	0.38	0.538
Reynolds number	1580	1280	921
Isp	304	301	298

Table.4

Reference

[1].Jahn.R.G.:Physics of Electric Propulsion (1968)

[2].Curra,F.M. and Sarmient,C.J. :Low Power Arcjet Thruster Performance Characterization AIAA Paper 90-2578(1990)

[3].K-Ogiwara,T-Yamada,K-Toki,K-Kuriki :Experiment of 300W-class Arcjet Thruster, ISTS 94-a-50(1994)